

JET-P(90)66

P-H Rebut
and JET Team

Future Prospects for JET and Next Step Tokamaks

“This document contains JET information in a form not yet suitable for publication. The report has been prepared primarily for discussion and information within the JET Project and the Associations. It must not be quoted in publications or in Abstract Journals. External distribution requires approval from the Publications Officer, JET Joint Undertaking, Abingdon, Oxon, OX14 3EA, UK”.

“Enquiries about Copyright and reproduction should be addressed to the Publications Officer, EFDA, Culham Science Centre, Abingdon, Oxon, OX14 3DB, UK.”

The contents of this preprint and all other JET EFDA Preprints and Conference Papers are available to view online free at www.iop.org/Jet. This site has full search facilities and e-mail alert options. The diagrams contained within the PDFs on this site are hyperlinked from the year 1996 onwards.

Future Prospects for JET and Next Step Tokamaks

P-H Rebut
and JET Team*

JET-Joint Undertaking, Culham Science Centre, OX14 3DB, Abingdon, UK

** See Appendix 1*

Preprint of Paper to be submitted for publication in
Fusion Engineering and Design

Future Prospects for JET and Next Step Tokamaks

by

PH Rebut

JET Joint Undertaking, Abingdon, Oxon. OX14 3EA, UK.

ABSTRACT

Latest results from the JET tokamak, with beryllium as the first wall material facing the hot plasma, have shown substantial improvements in plasma purity and corresponding reductions in plasma dilution. This has allowed a fusion product ($n_D \tau_E T_i$) of $8-9 \times 10^{20} \text{m}^{-3} \text{skeV}$ to be reached (within a factor of 8 of that required in a fusion reactor), albeit only transiently. Even so, at high heating powers, an influx of impurities still limits the achievement of better performance and steady state operation.

A New Phase for JET is planned in which an axi-symmetric pumped divertor configuration will be used to address the problems of impurity control, plasma fuelling and helium ash exhaust in operating conditions close to those of a Next-Step tokamak with a stationary plasma of thermonuclear grade. The New Phase should demonstrate a concept of impurity control; determine the size and geometry needed to realise this concept in a Next-Step tokamak; allow a choice of suitable plasma facing components; and demonstrate the operational domain for such a device. With an efficient axi-symmetric pumped divertor, ignition should occur in a tokamak reactor of about 2 to 3 times the size of JET.

It seems prudent to envisage international collaboration on a Next Step Programme, which could comprise several complementary facilities, each optimised with respect to specific clear objectives. There could be two Next Step tokamaks, and a Materials Test Facility. Such a programme would allow division of effort and sharing of risk across the various scientific and technical problems, permit cross comparison and ensure continuity of results. A single Next Step device (such as the ITER Project as currently conceived) has higher scientific, technical and management risks and does not provide such comprehensive information, particularly in the areas of ignition, reactor performance and blanket testing. Further details of these facilities, expected costs and timescales are discussed.

1. INTRODUCTION

The Joint European Torus (JET) is the central project in the European Fusion programme. This programme is coordinated by the European Atomic Energy Community (EURATOM). The EURATOM Fusion Programme is designed to lead ultimately to the construction of an energy producing reactor. Its strategy is based on the sequential construction of major apparatus such as JET, the next European Torus (NET), and DEMO (a demonstration reactor), supported by medium sized specialized tokamaks.

The objective of JET is to obtain and study a plasma in conditions and dimensions approaching those needed in a thermonuclear reactor [1,2] involving four main areas of study:

- (i) various methods of heating plasmas to the thermonuclear regime;
- (ii) the scaling of plasma behaviour as parameters approach the reactor range;
- (iii) the interaction of plasma with the walls and methods of fuelling and exhausting the plasma;
- (iv) the production of alpha-particles generated in the fusion of deuterium and tritium and the consequent heating of plasma by these alpha-particles.

JET is now in the second half of its experimental programme. The technical design specifications of JET have been achieved in all parameters and exceeded in several cases (see Table I). The plasma current of 7MA and the current duration of up to 30 seconds are world records and are more than twice the values achieved in any other fusion experiment. The neutral beam injection (NBI) heating system has been brought up to full power (~21MW) and the ion cyclotron resonance frequency (ICRF) heating power has been increased to ~18MW in the plasma. In combination, these heating systems have provided 35MW power to the plasma.

During its experimental programme, JET has devoted particular attention to studying the interaction of the plasma with the vessel walls. This paper summarises results obtained when JET was operated with carbon and then with beryllium as the first-wall to provide a low-Z material facing the plasma. Even though impressive results were obtained, at high heating powers, an influx of impurities still limits the achievement of better performance and prevents the attainment of steady state. A planned New Phase for JET [3] is presented: an axi-symmetric pumped divertor configuration would be used to address the problems of impurity control, plasma fuelling and helium ash exhaust in operating conditions close to those of a Next-Step tokamak with a stationary plasma of thermonuclear grade. Finally, the requirements for a Demonstration Fusion Reactor are set out and proposals are made on how international collaboration on a Next Step programme could be envisaged. This should comprise several complementary facilities, each optimised with respect to specific clear objectives.

2. JET SCIENTIFIC RESULTS AND ACHIEVEMENTS

The performance of JET, as indicated by the fusion triple product ($n_D n_T \tau_E T_i$), has increased significantly since beryllium was introduced into JET as a first-wall material, in two different ways: initially as a thin evaporated layer on the carbon walls and limiters; and later, in addition as a limiter material. The consequence of these different regimes of operation on each plasma physics parameter in the fusion triple product is detailed below. Of particular significance is the effect of improved plasma purity, which previously, with a carbon first-wall, had impeded progress towards a reactor.

Recently, it became apparent that impurities and density control were the main obstacles to improved JET performance. Graphite components had been developed to mechanically

withstand the power loads encountered. However, the interaction of the plasma with these components, even under quiescent conditions, caused unacceptable dilution of the plasma. In addition, imperfections in the positioning of the components led to localised heating during high power which caused enhanced impurity influxes. These influxes produced a condition called the 'carbon catastrophe', in which the plasma concentration, plasma temperature and neutron yield collapsed.

Density: With a carbon first-wall, the plasma density was limited. In general, this occurred when the radiated power reached 100% of the input power, leading to the growth of MHD instabilities and ending in a major disruption. The density limit was dependent on plasma purity and power to the plasma.

With a beryllium first-wall, the maximum operating density increased significantly by a factor of 1.6 - 2. A record central density of $4 \times 10^{20} \text{m}^{-3}$ was achieved by strongly peaking the density profile using a sequence of 4mm frozen deuterium pellets injected at intervals throughout the current rise phase of an X-point discharge. Moreover, the density limit increased with increasing total input power, approximately as the square root of the power (see Fig.1). Furthermore, the nature of the density limit changed and the frequency of disruptions at the density limit were much reduced. Disruptions did not usually occur, and the limit was associated rather with the formation of a poloidally asymmetric, but toroidally symmetric radiating structure (a "MARFE"), which clamped the plasma density. These results constitute a substantial enhancement of the operating capability of JET.

Experiments were performed in which heating and fuelling were varied systematically, using NBI, ICRF, gas and pellet fuelling. With pellet injection and additional heating, more peaked density profiles were established. Pellet fuelled discharges at the same edge density as gas fuelled discharges had considerably higher central densities. Fig.2 shows density profiles just before a density limit MARFE occurred (cases (a) and (b)) and far away from the density limit (case (c)). Density profiles are very similar near the edge, but the gas fuelling profile is remarkably flat. These flat profiles are difficult to reconcile with an anomalous particle pinch and pose important questions related to particle transport, and in particular, the transport and exhaust of helium ash products. With deep pellet fuelling and additional heating, peaked profiles are obtained (cases (a) and (c)). These studies suggest that the edge density may be correlated with the density limit which, under beryllium conditions, may be considered as a limitation of edge fuelling. These observations endorse the view that the density limit is determined by a power balance at the plasma edge. This suggests that the cause of disruptions is related to radiation near the $q=2$ surface. Furthermore, when the radiation is low, or confined to the outermost edge, there are no density limit disruptions.

Operation with beryllium gettering allowed improved density control (due to high wall pumping). A beryllium first-wall offered the additional advantages of improved plasma purity and reduced radiation. These factors allowed higher input powers, greater fuel concentrations

(n_D/n_e) (see Fig.3.) and improved fusion performance. On the longer timescale (minutes to hours), very little deuterium was retained in comparison with a carbon first-wall; over 80% of the neutral gas admitted to JET is recovered, compared to about 50% with a carbon first-wall. This has important advantages for the tritium phase of JET operation.

Temperature: High ion temperatures have been obtained at the low densities possible with a beryllium first-wall and with the increased neutral beam penetration afforded by operation at an energy of 140keV. Record ion temperatures were achieved: up to 18keV in material limiter plasmas and up to 30keV in magnetic limiter plasmas, for powers up to 17MW. A typical example is shown in Fig.4 in which the central ion temperature reached 28keV for about 15MW input in a magnetic limiter configuration. The ion temperature profile is sharply peaked and the electron temperature is significantly lower than the ion temperature, by a factor of 2-3. The central ion temperature is shown in Fig.5 to increase linearly with power per particle up to the highest temperatures so far achieved; the central electron temperature, on the other hand, is seen to saturate at about 12keV. At higher densities ($n_e(0) > 2 \times 10^{19} \text{m}^{-3}$), experiments with combined neutral beam and ICRF heating result in central ion and electron temperatures both exceeding 11keV in a 3MA plasma for an input power of 33MW (21MW NBI and 12MW ICRF heating).

Extensive studies have been performed in the 'monster-sawtooth' regime in which sawteeth oscillations have been suppressed for up to 5s by central ICRF heating. Peaked temperature profiles (with both central ion and electron temperatures above 10keV) were maintained for several seconds, which, in the equivalent D-T mixture, would result in a significant enhancement in the time-averaged fusion reactivity over that obtained in a sawtooth discharge.

These observations indicate that electron thermal losses are anomalous, with electron confinement degrading substantially with increasing input power. The ions, on the other hand, behave quite differently; although ion thermal transport is also anomalous, ion confinement degrades little with increasing input power. This suggests that the electrons are the fundamental cause of anomalous transport. This is in-line with the critical electron temperature gradient model for confinement [4].

Energy Confinement: With either a carbon or beryllium first-wall, the energy confinement time on JET improves with increasing current and decreases with increasing heating power, independent of the type of heating.

In the X-point configuration, H-modes [5] with high power heating (up to 25MW) have been studied. In comparison with limiter plasmas, the confinement is about a factor of two better, but the dependences on current and heating power are similar. Although the experiments with a beryllium first-wall were conducted with carbon X-point target plates and the confinement times were similar to those obtained with a carbon first-wall, better plasma purity

(central values of fuel concentration (n_D/n_e) were in the range 0.7-0.9) allowed substantially improved fusion performance.

With a carbon first-wall, H-modes with ICRF heating alone were not obtained; with a beryllium first-wall, H-modes were successfully obtained with ICRF heating alone. This was mainly possible because of beryllium evaporation onto the nickel antennae screens, which lead to a lower impurity production. With beryllium antennae screens, H-modes were achieved with either monopole or dipole phasing of the ICRF antennae. The confinement in H-modes with ICRF alone was similar to that with NBI.

In summary, the global confinement time degraded with input power for both ICRF and NBI heating in the range 4 - 25MW. The dependence of the confinement times on heating power in both material and magnetic limiter configurations is shown in Figs.6(a) and (b), respectively. Typically, H-mode confinement is about twice L-mode confinement.

These observations indicate that the transport in the H- and L-regimes are similar, except for an edge thermal barrier which is easier to establish with X-points and high shear. Furthermore, energy confinement does not appear to be affected by the impurity mix (carbon or beryllium in deuterium plasmas).

Beta Limits: Experiments have explored the plasma pressure (as represented by the β -value) that can be sustained in JET and investigated the plasma behaviour near the expected β -limit in a double-null H-mode configuration, at high density and temperature and low magnetic field ($B_t = 1$ T). Values of β_t up to $\sim 5.5\%$ were obtained. The β_t limit is close to the Troyon limit [6] $\beta_t(\%) = 2.8 I_p(\text{MA})/B_t(\text{T})a(\text{m})$, where I_p is the plasma current and a is the plasma minor radius, as shown in Fig.7. Significantly, it is found that the limit in JET does not appear to be disruptive. Rather, a range of magneto-hydrodynamic (MHD) instabilities occur and these limit the maximum value of β without causing a disruption.

The behaviour near both the density and β -limits may be reconciled in terms of resonant instabilities, which have the magnetic topology of islands.

Impurities: With a carbon first-wall, the main impurities in JET were carbon (2-10%) and oxygen (1-2%). With beryllium evaporation, oxygen was reduced by factors >20 , and carbon by >2 . Although beryllium increased, carbon remained the dominant impurity for this phase. With beryllium limiters, the concentration of carbon was reduced by a further factor of 10, but beryllium levels increased by about a factor of 10, and became the dominant impurity. Due to the virtual elimination of oxygen, and the replacement of carbon by beryllium, impurity influxes were reduced significantly, in line with a model [7] which takes account of impurity self-sputtering. As shown in Fig.3, it had not been possible to maintain (n_D/n_e) much above 0.6 with carbon limiters even for moderate input powers, but values greater than 0.8 were routinely achieved with beryllium limiters. Correspondingly, the effective ionic charge, Z_{eff} , was

reduced significantly, already with the beryllium evaporation, and then more so with beryllium limiters. Z_{eff} as a function of line density for the three phases of operation is shown in Fig.8.

The improved plasma purity contributes significantly to improved fusion performance, which otherwise could be achieved only with a substantial increase in energy confinement.

Fusion Performance: The use of beryllium resulted in the elimination of oxygen, the reduction in the carbon influx and the increase in the plasma purity, with the fuel concentration (n_D/n_e) increasing to 0.9. Since the X-point tiles remained as carbon, the carbon catastrophe was not affected significantly with a beryllium first-wall. However, the duration of the H-mode was extended by up to 50% either by sweeping the X-point (both in the radial and vertical directions) to reduce the X-point tile temperatures, or by using strong gas puffing in the divertor region. Improved plasma purity and increased ion temperatures ($T_i(0)$ in the range 20 - 30keV) resulted, leading to improved plasma performance. In a particular case, the central ion temperature reached 22keV, the energy confinement time, τ_E , was 1.1s, with a record fusion product ($n_D(0)\tau_E T_i(0)$) of $8-9 \times 10^{20} \text{m}^{-3} \text{skeV}$. The neutron yield for this discharge was also the highest ever achieved on JET at $3.5 \times 10^{16} \text{ns}^{-1}$, with $Q_{DD} = 2.4 \times 10^{-3}$. A full D-T simulation of this pulse showed that 12MW of fusion power could have been obtained transiently with the 16MW of NBI, giving a fusion product value ($n_D\tau_E T_i$) within a factor of 8 of that required in a reactor. The overall performance of the fusion product, as a function of ion temperature, T_i , is shown in Fig.9. for a number of tokamaks.

Summary of Scientific Achievements: Substantial progress has been made with beryllium as a first-wall material, affecting impurity influxes such that:

- oxygen impurities were essentially eliminated;
- the effective ionic charge, Z_{eff} , was significantly reduced in ohmic plasmas (down to 1.2) and with strong additional heating (down to <1.5);
- a severe carbon influx ('carbon catastrophe') persisted for inner wall and X-point plasmas, and represents a serious limitation in H-mode studies.

Reduced impurity levels allowed prolonged operation at higher densities and improved the general JET performance, as follows:

- the pumping of deuterium with a beryllium first-wall was more efficient than with a carbon first-wall and provided improved density control. This permitted low density and high temperature (up to 30keV) operation for times >1s;
- the density limit increased, with a record peak density of $4 \times 10^{20} \text{m}^{-3}$ with pellet fuelling. This limit is principally a fuelling limit and not a disruption limit, as found with carbon limiters;
- sawtooth free periods exceeding 5s were achieved, but the stabilisation mechanism remains unclear.

- H-modes of 1s duration were created with ICRF heating alone. Their confinement characteristics were similar to those with NBI heating alone;
- β values up to the Troyon limit were obtained in low field double-null X-point plasmas;
- the neutron yield doubled to $3.5 \times 10^{16} \text{s}^{-1}$ and the equivalent fusion factor Q_{DT} increased to ~ 0.8 ;
- the fusion product ($n_D \tau_E T_i$) increased to $8\text{-}9 \times 10^{20} \text{m}^{-3} \text{skeV}$ for both high ($>20 \text{keV}$) and medium temperatures (9keV), reaching near breakeven conditions and was within a factor of 8 of that required in a reactor.

However, the results were obtained only **transiently** and could not be sustained in a steady state. Ultimately, the influx of impurities caused a degradation in plasma parameters.

3. IMPURITY CONTROL: A PLANNED NEW PHASE FOR JET

So far, JET has concentrated on **passive** methods of impurity control, reducing impurity production by proper choice of plasma-facing components (such as beryllium or beryllium carbide), sweeping the magnetic configuration across the target plates and benefitting from the formation of a highly radiating zone in front of the target plates. Studies of **active** impurity control represent a natural development of the JET programme and accordingly, a New Phase for JET is planned to start in 1992 [3], with first results becoming available in 1993 and continuing to the end of 1996.

The aim of the New Phase is to demonstrate, prior to the introduction of tritium, effective methods of impurity control in operating conditions close to those of a Next Step tokamak, with a stationary plasma of 'thermonuclear grade' in an axisymmetric pumped divertor configuration. Successful impurity control would lead also to an increase in alpha-particle power by more than a factor of two.

Specifically, the New Phase should demonstrate:

- the control of impurities generated at the divertor target plates;
- a decrease of the heat load on the target plates;
- the control of plasma density;
- the exhaust capability;
- a realistic model of particle transport.

Principal concepts of active impurity control

Since the sputtering of impurities at the target plates cannot be suppressed, such impurities must be retained close to the target plates for effective impurity control. This may be achieved by friction with a strong plasma flow directed along the divertor channel plasma (DCP) towards the target plates [8]. The plasma flow will be generated by a combination of gas puffing, the injection of low speed pellets and the recirculation of some of the flow at the target plates

towards the X-point. The connection length along the magnetic field line between the X-point and the target plates must be sufficiently long to allow effective screening of impurities.

Hypervapotron elements will be used for the high heat flux components of the target plates, and these are expected to accommodate power fluxes up to 15MWm^{-2} at the copper-beryllium interface. Of course, rapid sweeping (4Hz) of the target plates to limit the localised heat load, to limit erosion and to affect redeposition will be important. Methods of ensuring that a substantial fraction of input power can be radiated in a controlled way in the DCP will be key features.

In the vicinity of the target plates, a pumping chamber (with a cryo-pump) is introduced to control the main plasma density by exhausting and pumping a relatively large fraction $\sim 10\%$ of the plasma flow created by fuelling. The fuelling and exhaust capability of a Next Step will be dependent on whether deuterium and impurities (including helium ash) accumulate in the plasma centre. The production and transport of helium ash towards the plasma edge (where it must be exhausted) will depend on the relative importance of energy and particle confinement (D/χ ratios), the effect of sawteeth and the effect of an edge transport barrier forming in the H-mode. To assess fully these issues requires detailed modelling of particle transport and while this forms already an important part of present JET studies, a substantial experimental and modelling effort is envisaged for the New Phase.

Modelling Impurity Control

The plasma behaviour in the scrape-off-layer (SOL) and divertor channel plasma (DCP) can be understood qualitatively by considering the basic steady state equations for the particle flux, F , and the total plasma pressure, p , along the magnetic field line direction, x . Fig.10 shows isothermals and isoflows in the pressure (p) versus impurity density (n_z) plane. These curves intersect at two points, above and below a pressure $p_0/2$, corresponding to subsonic and supersonic flows, respectively. For a given plasma temperature, the maximum isoflow compatible with the steady state momentum equation is tangent to the isothermal at $p_0/2$.

Impurity retention in the divertor is determined from the steady state momentum equation for impurity ions, which for the simplest, realistic case gives the impurity density, n_z , decaying exponentially with distance from the target on a scale length, λ_z , given by

$$\lambda_z^{-1} = \lambda_F^{-1} - \lambda_e^{-1}, \quad \text{with} \quad \lambda_F^{-1} = \frac{m_z v_z}{T \tau_z} \quad \text{and} \quad \lambda_e^{-1} = \alpha_z \frac{1}{T} \frac{dT}{dx}$$

The temperature gradient scale length is given by the heat transport equation with electron heat conductivity parallel to the magnetic field ($\kappa = \kappa_0 T^{5/2}$) being dominant and is primarily dependent on the input power. To ensure impurity control, the frictional force must exceed the sum of the pressure and thermal forces, that is, $\lambda_F^{-1} > \lambda_e^{-1}$.

A high density, low temperature plasma in front of the target plates increases the friction between the hydrogen and impurity flows and facilitates impurity control [8]. Furthermore,

such a plasma limits the surface erosion and thereby increases the lifetime of the target plates. However, such operation will lead to high densities at the separatrix and this will be unfavourable for non-inductive current drive using neutral beams or lower hybrid waves.

To solve the full set of classical fluid equations for the conservation of particles, momentum and energy in the SOL and DCP, a numerical 1-1/2 D transport model has been developed. Monte Carlo methods are used for neutral particles in the flux surface geometry of the planned pumped divertor configuration. The model shows that impurities can be retained near the target plates for plasma flows, typically $\sim 10^{23}\text{s}^{-1}$. The steady state distribution of beryllium impurities, for conditions with and without flow, are shown in Fig.11.

The Pumped Divertor Configuration

The aims of the New Phase can be realised with the internal multi-coil configuration shown in Fig.12. The design allows a large plasma volume at 6MA and the operational flexibility to modify the magnetic configuration in the vicinity of the X-point independent of the plasma current and separately on the high and low field sides. In contrast to the normal configuration for a divertor, all divertor coils carry current flowing in the same direction as the plasma current. With this configuration, single null X-point operation is possible for performance and impurity control studies, including plasmas with 6MA for 10s, a volume $\sim 93\text{m}^3$ and a connection length from the X-point to the target plates of 3m and with 5MA for 10s, a volume $\sim 80\text{m}^3$ and a connection length $\sim 10\text{m}$. In addition, it should be possible to run 3MA double null X-point plasmas for up to 20s at 3.4T and for up to 1 minute at 2.1T.

4. REQUIREMENTS FOR A DEMONSTRATION FUSION REACTOR

Fusion Research Programmes are directed ultimately to the construction of a Demonstration Fusion Reactor - DEMO. From physics considerations and present technology constraints, the size and performance of a thermonuclear reactor can be largely defined. The minor radius of the plasma needs to be twice as large as the tritium breeding blanket thickness, so it must be $\sim 3\text{m}$ and the elongation can be as large as 2. Therefore, there is no need to operate at a toroidal field greater than 5T, in order to fulfil the plasma physics requirements. A practical aspect ratio of 2.5 sets the plasma major radius to 8m. Safe operation can be assumed for a cylindrical safety factor 1.6-1.8. This defines a reactor with a plasma current of $\sim 30\text{MA}$. Such a DEMO would produce power in the range 3-6GW thermal or 1-2GW electrical power.

The construction of a DEMO must be preceded by an extensive test of the concepts and technologies needed for incorporation into a DEMO design. In particular, tests and developments of plasma facing components and first-wall materials with a high resilience to 14MeV neutron radiation at a power flux of $2\text{-}3\text{MWm}^{-2}$ must be carried out in parallel with tests and developments of divertor target materials with high power handling capability and low erosion (eg. low Z materials, beryllium, carbon and carbide fibres, silicon carbide). The

concept of a D-T fuelling system with a high speed pellet injector ($v \geq 10 \text{ km/s}$) would need to be demonstrated. In the areas of helium ash exhaust, pumping and the divertor configuration, besides the forthcoming tests in the New Phase of JET, progress is still needed to prove the viability of present or emerging concepts. Tritium breeding blankets are required to operate at high temperatures and have not yet been tested. Furthermore, in the area of superconducting technologies, viable high critical temperature superconducting materials are desirable for sufficient safety margins and these need thorough testing. Finally, a credible physics concept still needs to emerge for current drive, to sustain continuous plasma operation. However, this last requirement may prove to be unnecessary when semi-continuous operation (~ 2 hours) has been demonstrated, which maybe sufficient for a commercial reactor.

In view of the time needed to develop and incorporate emerging technologies required for a DEMO, a precisely defined or optimised engineering design cannot yet be proposed. A reasonably broad strategy would be to develop, partly in parallel, the main components of a fusion reactor. More than one DEMO seems desirable (as in the early development of fission). The Next Step needs to address all the physics and technological issues of a DEMO device.

5. THE NEXT STEP

The Next Step will provide the bridge from present devices to the position from which DEMO could be designed and constructed. As such, the aim of the Next Step is to demonstrate the scientific feasibility of ignition under conditions required for a DEMO device: that is, high power long pulse operation in fully ignited plasmas ($Q_{DT} = \infty$). It is also necessary to test hot blanket modules and the resistance of highly sensitive materials (eg insulators, first-wall) to high neutron fluences. Furthermore, semi-continuous or continuous operation and the viability of a fully superconducting tokamak must be demonstrated.

The variety of issues that the Next Step must address are expected to mature on different timescales. A single facility whose objectives cover all issues will have an unacceptable risk of failure unless a large safety margin is allowed on each component. In addition, it would not allow cross comparison of results nor permit continuity of data flow. To incorporate all innovations that are likely to reach maturity throughout the lifetime of a single facility requires a design which lacks the precise definition offered by well targeted objectives. There would also be an impact on the starting and construction times and on the consequential costs. A large degree of complexity would be introduced and this would place a practical limit on intended flexibility. A reactor strategy which would minimise risks and costs would be to address the different Next Step issues in several complementary facilities, each with separate objectives. This strategy requires a clearly defined Next Step **Programme** rather than a **single device**.

In such an optimised Next Step Programme, the three main issues of long burn ignition, superconducting coil technology and material testing are separated and addressed in three different facilities (P1, P2, P3) which are constructed on a timescale commensurate with the

maturities of the technologies. The engineering design for each facility can be defined precisely, thereby allowing a high degree of confidence that objectives would be met.

The main details of such machines are the following:

- The primary objectives of P1 would be:
 - to demonstrate sustained high power operation of a fusion reactor core of 2-3GW thermal power produced for up to 12hrs per day for periods up to 6 days at a time;
 - to provide a testbed for the study and validation of tritium breeding blanket modules in full reactor conditions;
 - to achieve a cost/unit thermal output relevant to the establishment of fusion as a potential economic energy source (1ECU/thermal Watt).

The design philosophy of P1 would be:

- to make full use of the scientific and technical experience gained from JET and the rest of the tokamak programme;
- to minimise the need for developments by using established techniques;
- to reduce complexity and increase reliability at reasonable cost;
- to provide a high safety margin in achieving design specifications for the magnetic field and plasma current.

As a consequence, conventional coil technology could be used and this would allow an early start in 1994 once the results on impurity control become available from the New Phase of JET. These objectives could be achieved in a tokamak with 30MA, 4-5T, major radius 8m, minor radius 3m, and elongation of 2. Impurities would be controlled actively by high density operation and a pumped divertor. The approach to ignition would utilise ICRF heating with H-mode confinement and in the monster sawtooth regime, while long pulse ignition (> 30 mins) would be sustained with L-mode confinement at high power and also with high frequency low amplitude sawteeth. With sustained ignition conditions, blanket modules would be tested under neutron fluxes of up to 2MWm^{-2} .

- The primary objectives of P2 would be:
 - to demonstrate the viability of high power operation of a large tokamak with superconducting magnets;
 - to assess continuous operation at high density with current drive;
 - to assess profile control;
 - to assess advanced divertor concepts.

The design philosophy would be to test, at a reasonable cost, superconducting and non-inductive current drive technologies in a low activation environment, so that flexibility could be built-in to incorporate innovations for concept development throughout the lifetime of the device. Some technological developments are still required and therefore, construction could start somewhat after P1, perhaps in 1998. The P2 objectives could be realised with a large tokamak operating at high power typically 10-12MA, 6-7T, minor radius 1.5m, major radius 5m, and elongation of 2. To control the density and

impurities, an advanced exhaust and divertor concept would be used. To minimise activation, the tokamak would not operate in tritium and therefore would not ignite.

- The objective of P3 would be to test materials under very large neutron fluences. This could be realised in a test bed operating continuously and providing high fluxes of neutrons ($2-10 \text{ MWm}^{-2}$) over surfaces of $0.04-0.05\text{m}^2$. Its construction could start early in 1998, so that results should be available for the design of a DEMO in 2005.

A schedule for the design construction, and operation of Next Step and DEMO devices is shown in Table II. The overall cost for such a minimum Next Step Programme is estimated at 7bnECU, not including operation costs. This is similar to the cost of a single ITER device. However, for this cost, a single device would not cover all the issues of the Programme. Furthermore, the programme offers flexibility in location of the different facilities and in their starting dates.

6. CONCLUSIONS

- JET has successfully achieved or surpassed its original design aims and in doing so has produced and contained plasmas of thermonuclear grade.
- **Individually**, each of the parameters n , τ_E and T_i required for a fusion reactor have been achieved; **simultaneously**, the fusion product of these parameters is within a factor 8 of that required in a fusion reactor.
- However, these extremely good results were obtained only **transiently**, and were limited by impurity influxes due to local overheating of protection tiles.
- A New Phase is planned for JET, prior to the introduction of tritium, to demonstrate effective methods of impurity control in operating conditions close to those of a Next Step tokamak, with a stationary plasma of 'thermonuclear grade' in an axisymmetric pumped divertor configuration.
- Based on present progress, there is confidence that sufficient knowledge exists to begin the construction of the "core" of a fusion reactor within the next 3-4 years.
- However, a **single** Next Step facility (ITER) is a high risk strategy in terms of physics, technology and management, since **it does not provide a sufficiently wide base for a demonstration reactor.**
- A Next Step Programme comprising several facilities:
 - would make more effective use of resources;
 - is well within the capability of world research;
 - would provide a wider and more comprehensive data base; and
 - could even be accomplished without a significant increase in existing funding.
- With concerted effort and determined international collaboration, such a programme would provide sufficient results to allow the design of a DEMO to start in about 2005.

7. REFERENCES

- [1] The JET Project - Design Proposal: EUR-JET-R5
- [2] Rebut, P-H, et al, Fusion Technology, **11**, (1987), 13-281
- [3] Rebut, P-H, et al, JET Contributions to the Workshop on the New Phase for JET: The Pumped Divertor Proposal (September, 1989), JET Report - JET R(89)16
- [4] Rebut, P-H, Lallia, P, Watkins, ML, Proc. of the 12th Int. Conf. on Plasma Physics and Contr. Fusion Research (Nice, France, 1988), Nuclear Fusion Supplement (1989) Vol.2 p.191
- [5] Wagner, F, et al, Phys. Rev. Lett. **49**, (1982), 1408
- [6] Troyon, F, Gruber, R, et al, Plasma Phys. Controlled Fusion, **26**, (1984), 209
- [7] Summers, D.D.R., et al, J. Nucl. Mater., to be published (1990)
- [8] Neuhauser, J, et al, J. Nucl. Mat., **121**, (1984), 194

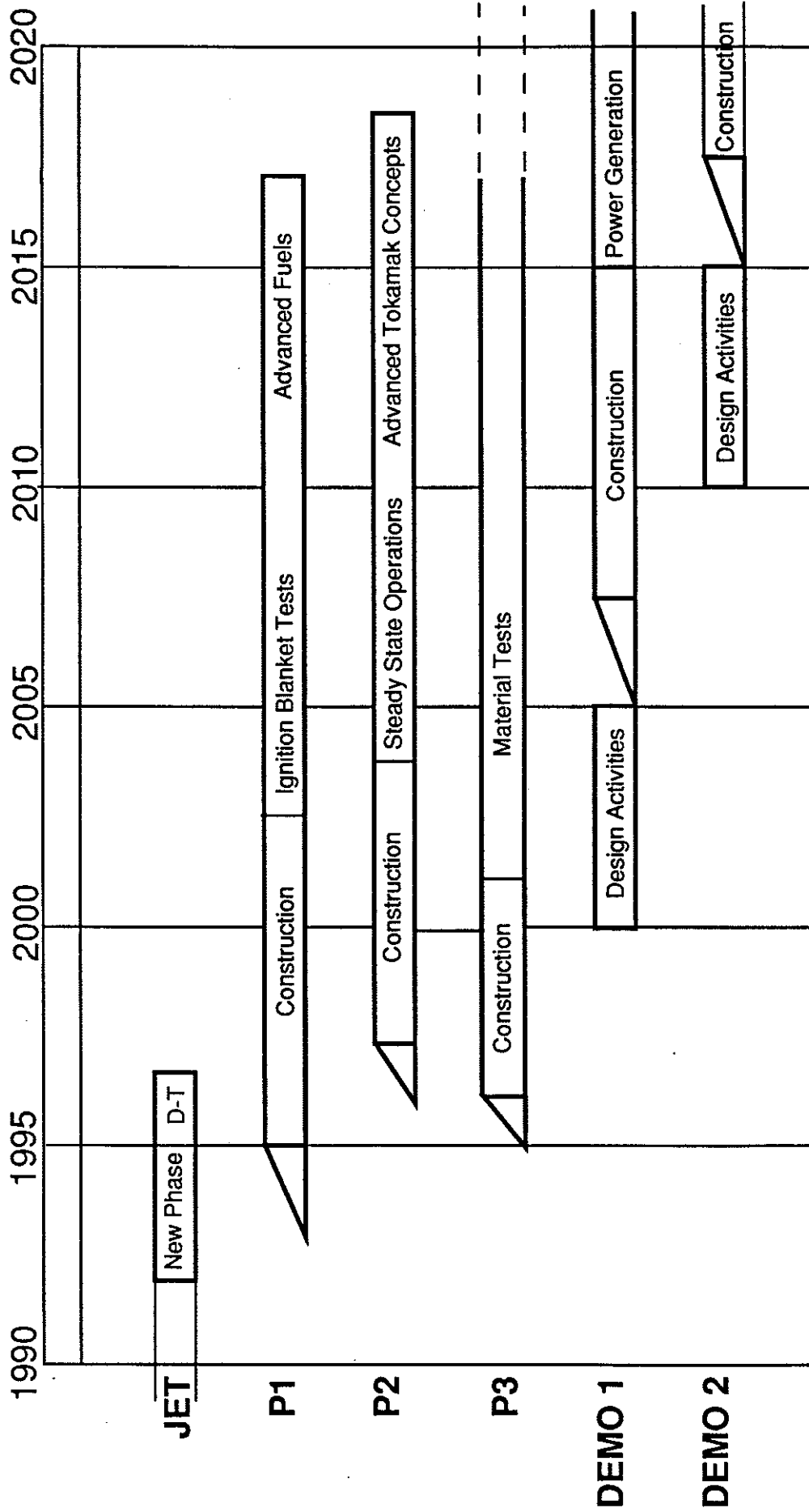
8. ACKNOWLEDGEMENTS

The author is indebted to Drs DJ Gambier, BE Keen and ML Watkins for assistance in preparation of the paper. In addition he is grateful to the JET Team, without whom the results in this paper would not be available.

Table I
JET Parameters

Parameters	Design Values	Achieved values
Plasma Major Radius (R_0)	2.96m	2.5-3.4m
Plasma Minor Radius horizontal (a)	1.25m	0.8-1.2m
Plasma Minor Radius vertical (b)	2.1m	0.8-2.1m
Toroidal Field at R_0	3.45T	3.45T
Plasma Current:		
Limiter mode	4.8MA	7.1MA
Single null X-point	not foreseen	5.1MA
Double null X-point	not foreseen	4.5MA
Neutral Beam Power		
(80kV, D)	20MW	21MW
(140kV, D)	15MW	8MW
		(only one box converted)
Ion Cyclotron Resonance		
Heating Power to Plasma	15MW	18MW

Table II: A Time Schedule for an ITER Programme



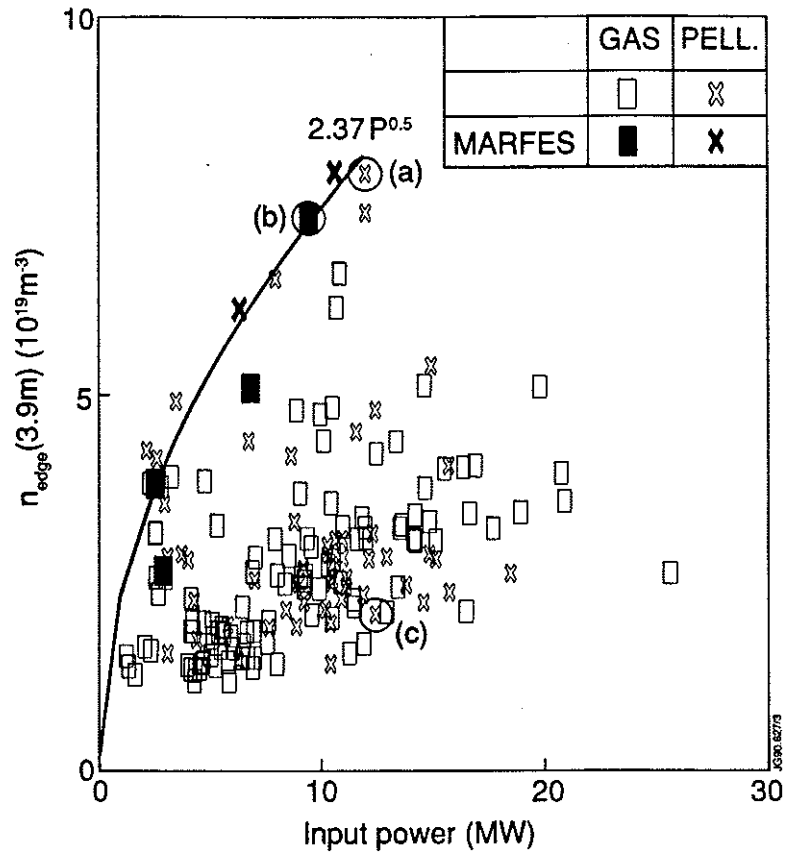


Fig 1 The edge electron density (n_{edge}) versus input power (P) showing that the density limit occurs at the boundary of the operational domain close to the curve $n_{\text{edge}} (\times 10^{19}\text{m}^{-3}) = 2.37 P^{1/2}(\text{MW})$. The profiles shown in Fig. 2 correspond to the three data points circled.

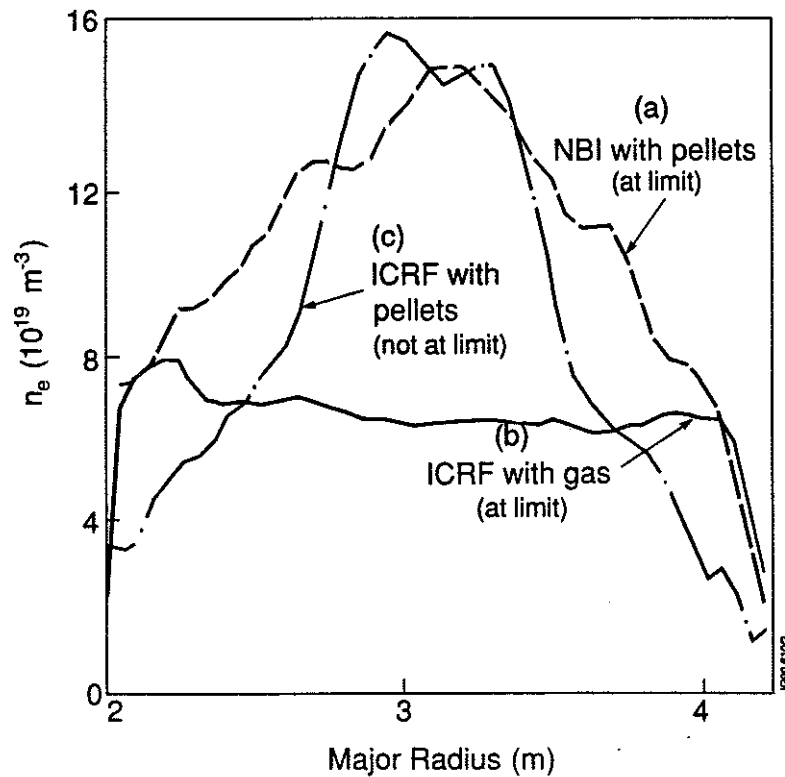


Fig 2 Electron density profiles for different fuelling and heating methods.

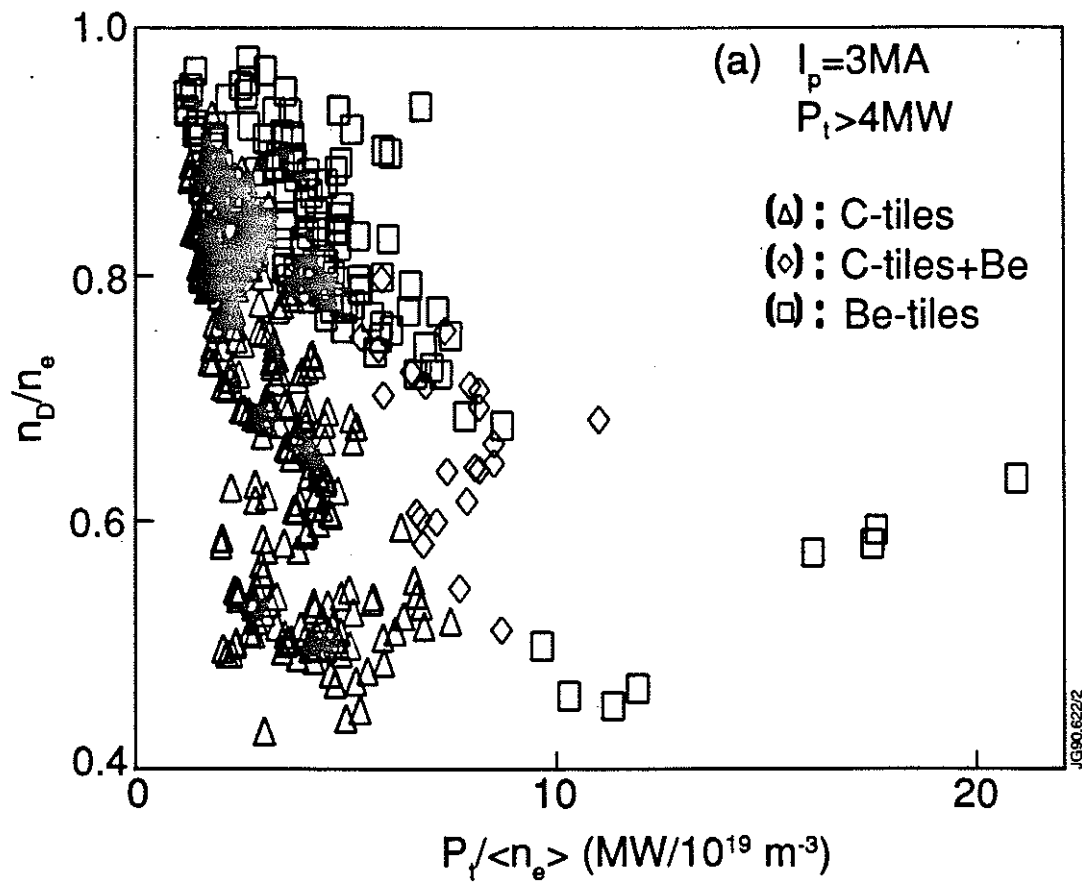


Fig 3 Fuel concentration, n_D/n_e , as a function of power per particle ($P_i/\langle n_e \rangle$) for carbon limiter tiles, beryllium gettering and beryllium limiter tiles.

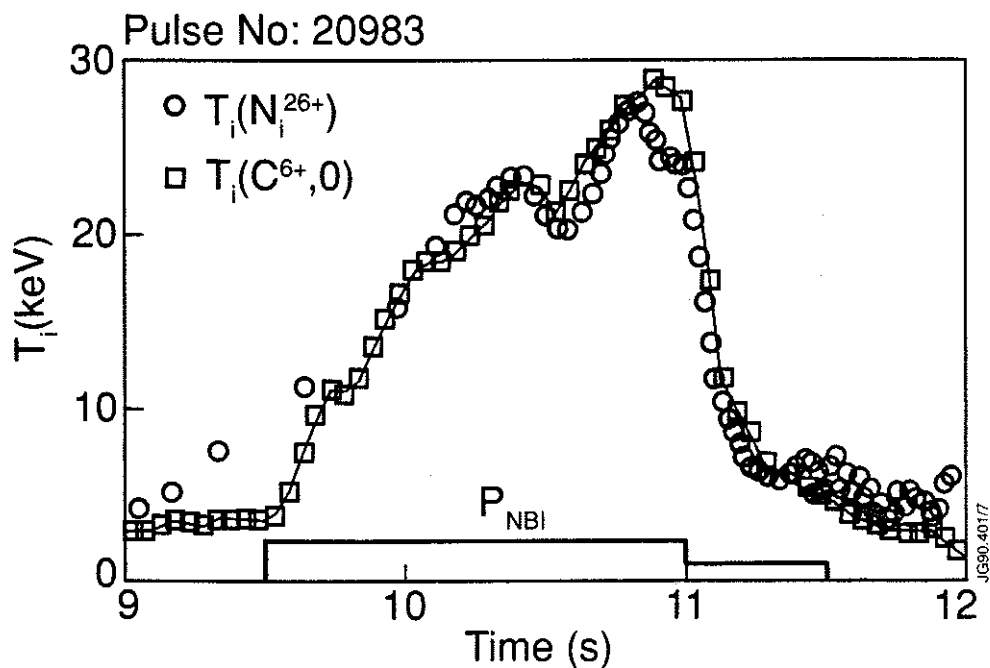


Fig 4 Ion temperature as a function of time during NB heating showing that temperatures of ~ 30 keV are reached.

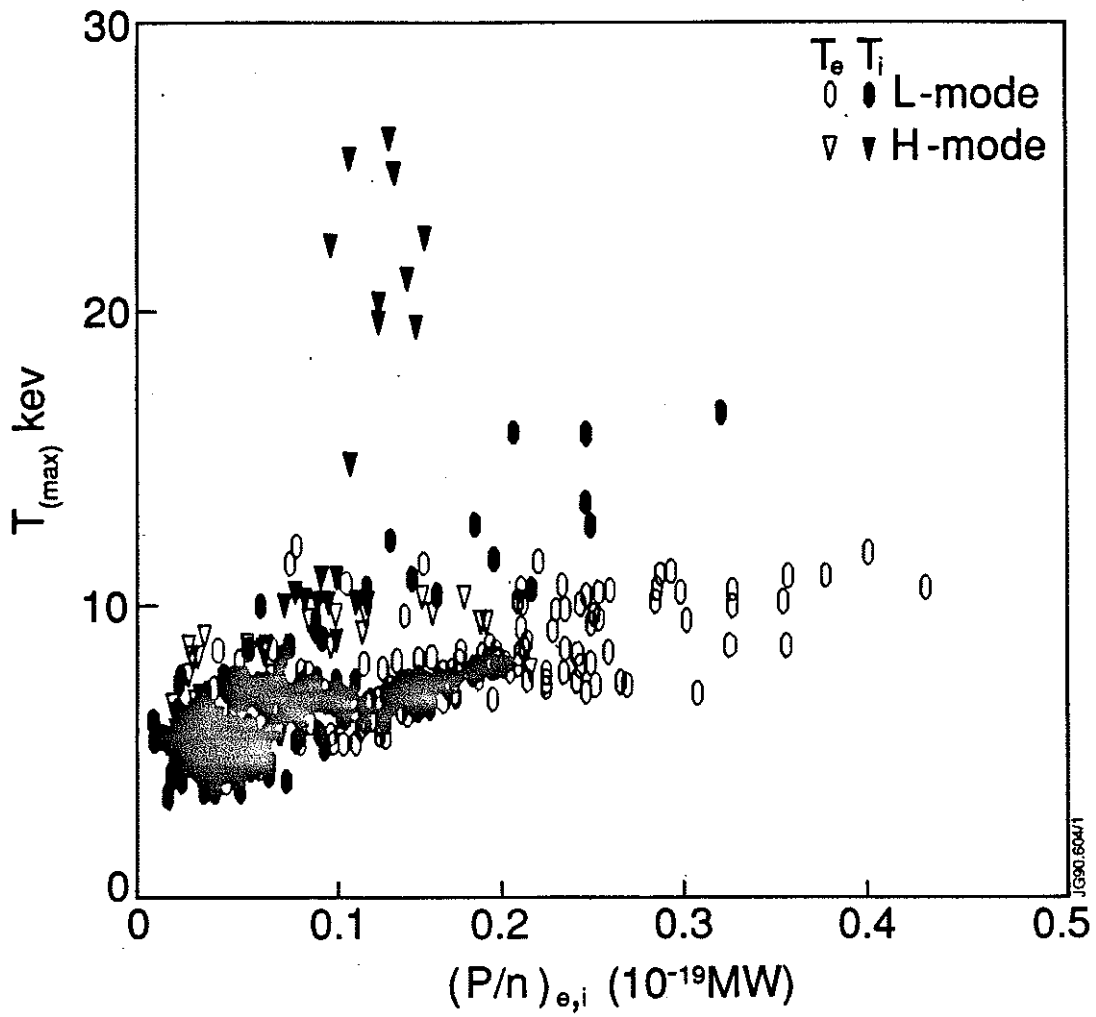


Fig 5 Central ion (T_i) and electron (T_e) temperatures as functions of power per particle $(P/n)_{e,i}$ to either species.

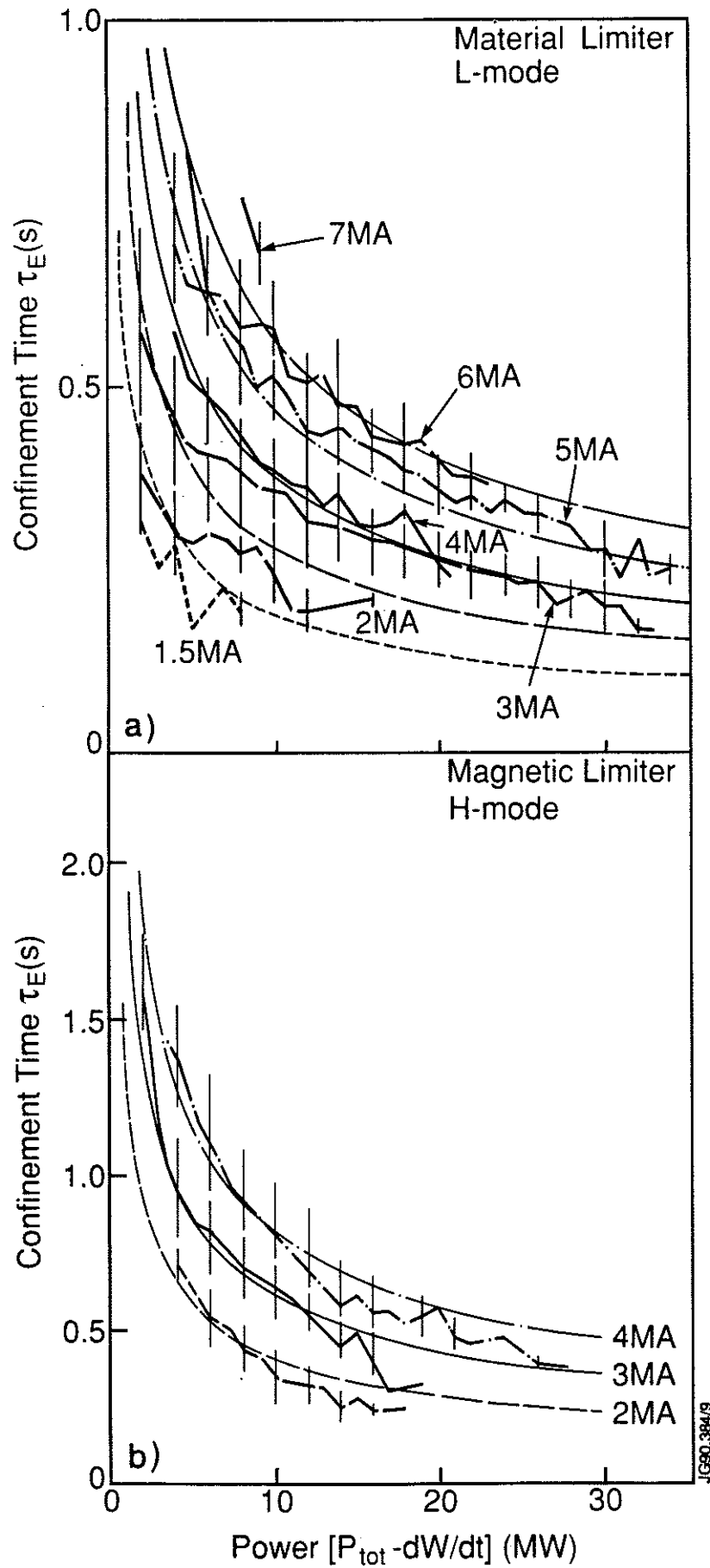


Fig 6 Global energy confinement time (τ_E) as a function of input power for (a) material limiters (L-mode) and (b) magnetic limiters (H-mode).

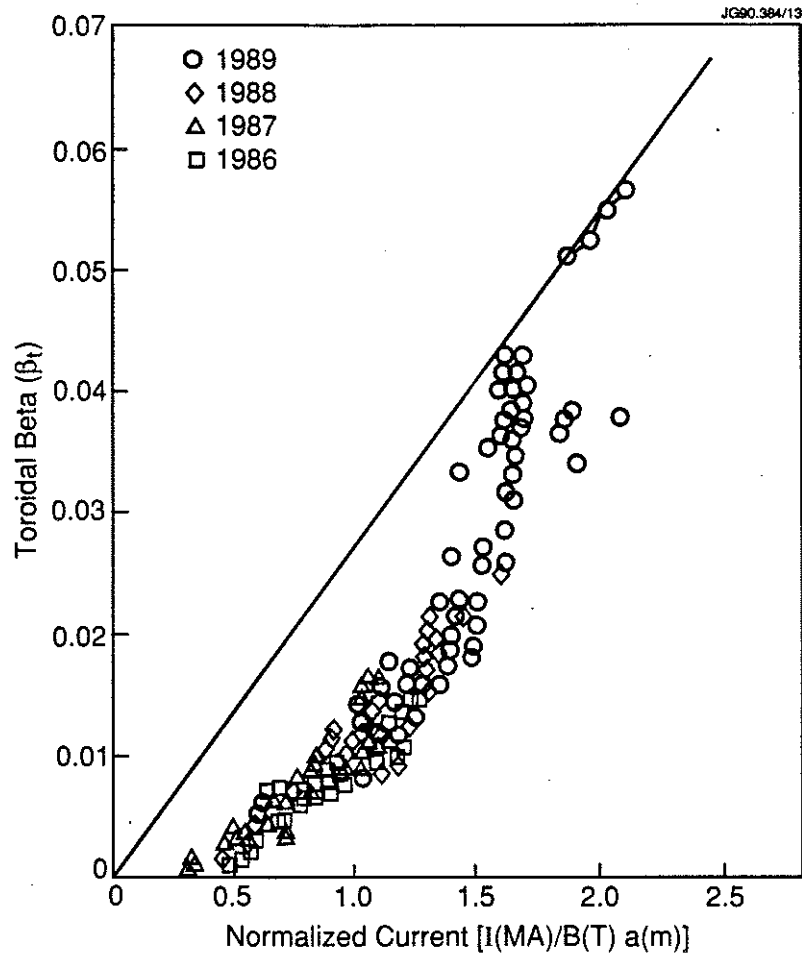


Fig 7 The maximum toroidal beta ($\beta_t=2\mu_0\langle p\rangle/B_t^2$) as a function of normalized current $I_p(\text{MA})/B_t(\text{T})a(\text{m})$.

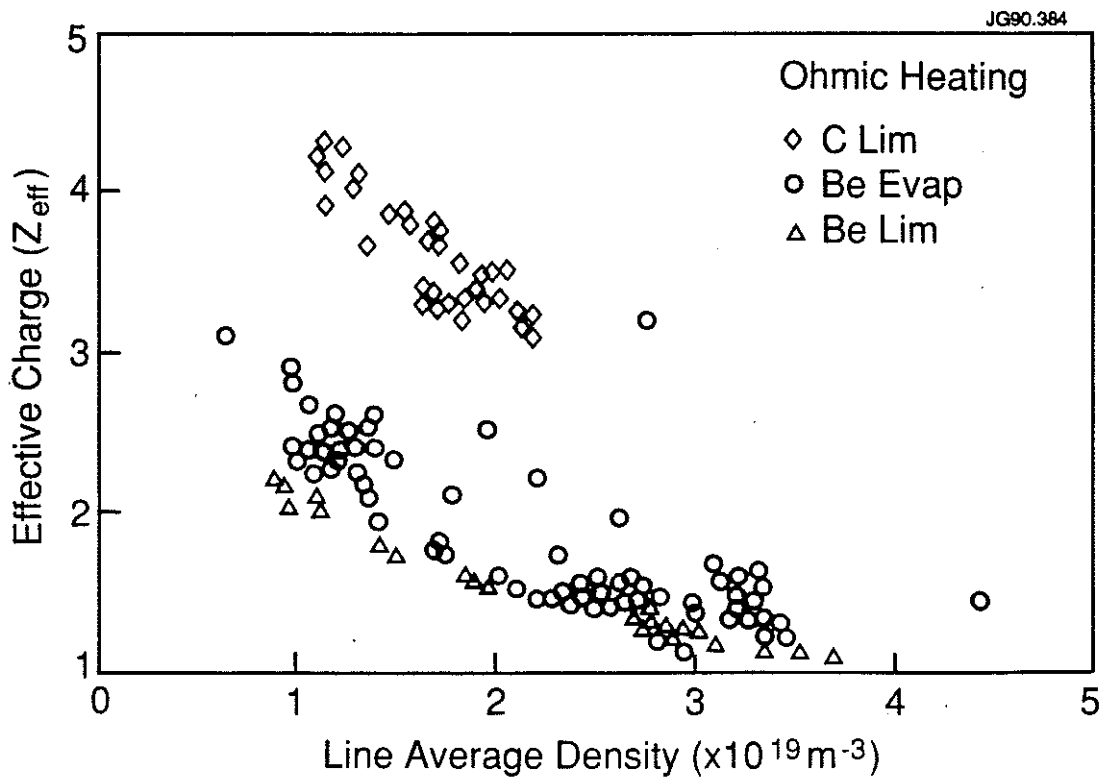


Fig 8 The effective ionic charge, Z_{eff} , as a function of line average density $\langle n_e \rangle$.

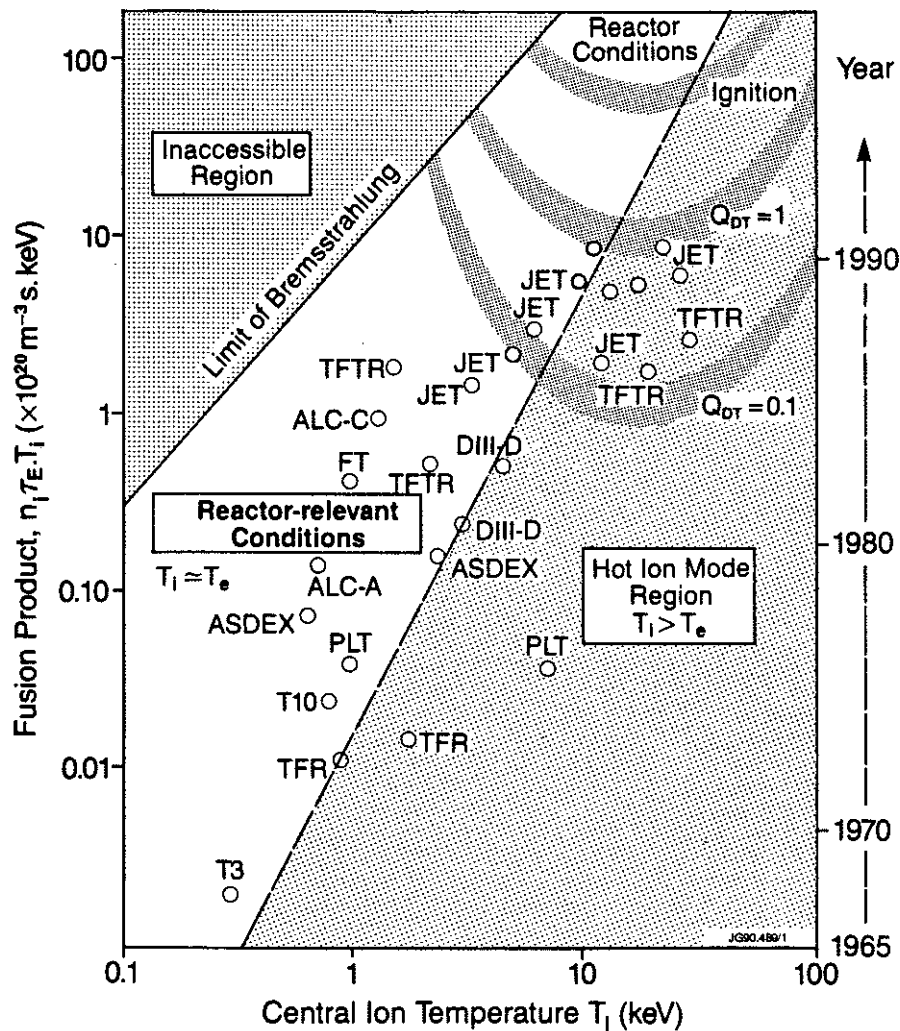


Fig 9 Overall performance of the fusion product ($n_D n_E T_i$) as a function of ion temperature (T_i), for a number of tokamaks.

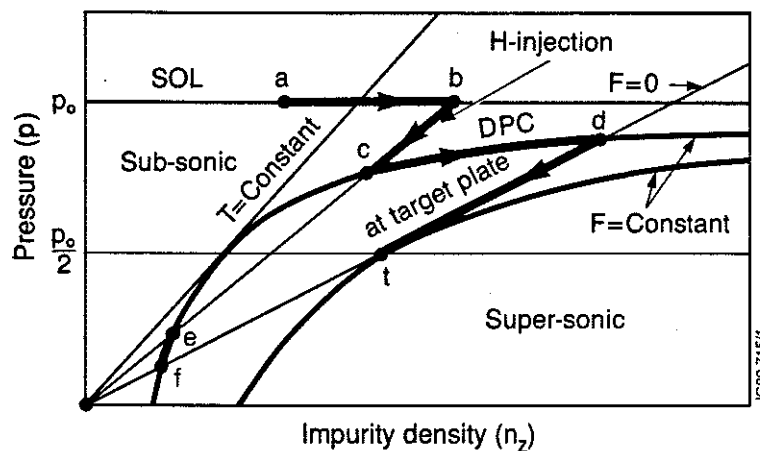


Fig 10 Diagram of pressure (p) versus impurity density (n_z) showing the qualitative behaviour of plasma parameters:

- in the SOL (section a-b where the flow $F=0$)
- at the X-point (section b-c)
- in the DCP (section c-d where $F = \text{constant}$)
- in front of the target plates (section d-t where the flow becomes transonic)

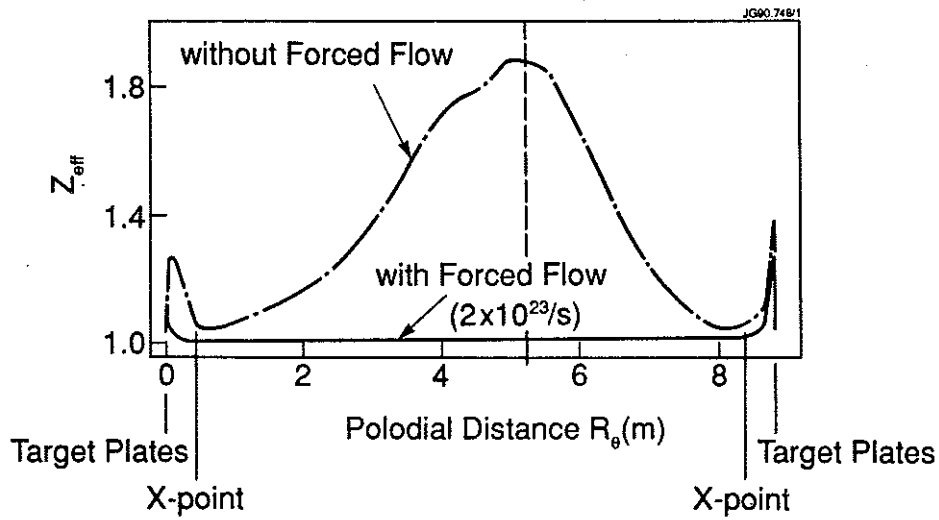


Fig 11 Poloidal distribution in the SOL and DCP between target plates of the effective ionic charge, Z_{eff} , for cases with and without flow

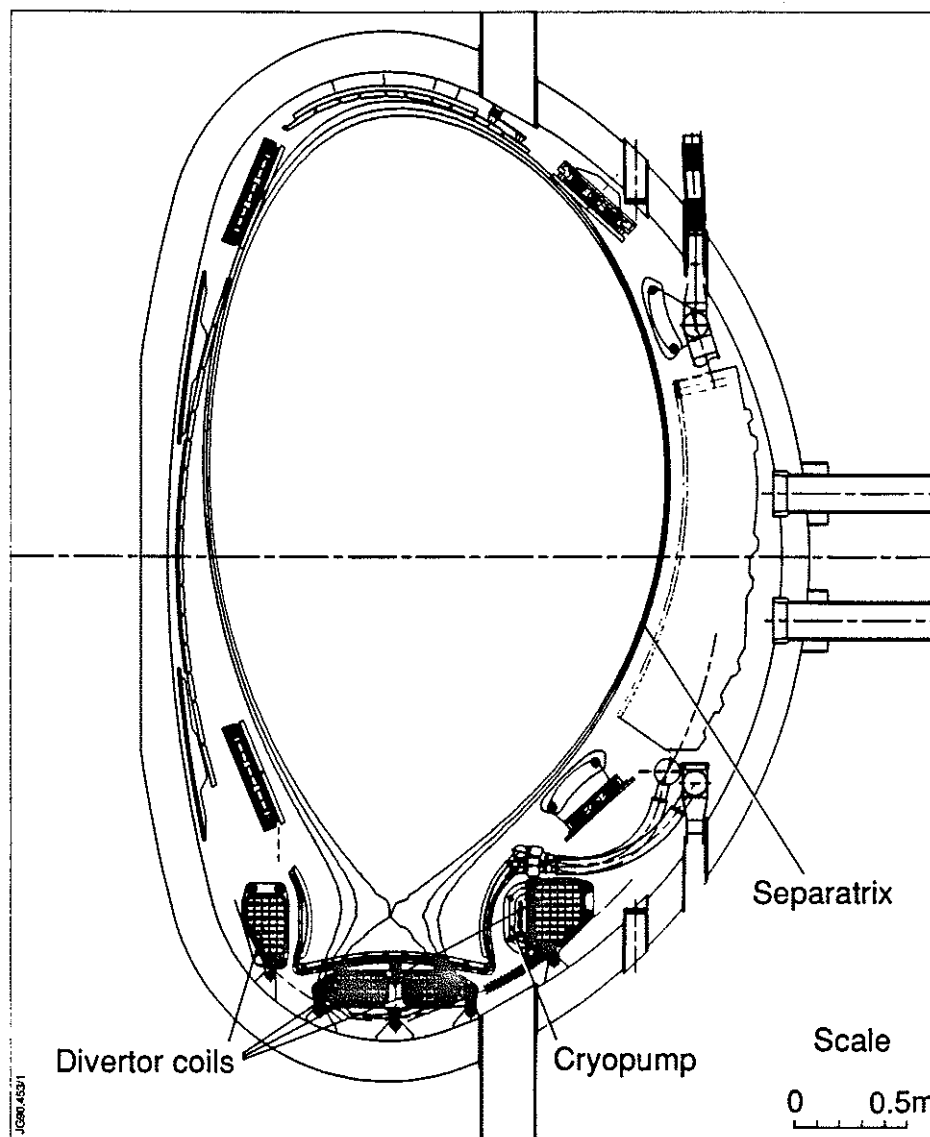


Fig 12 Poloidal cross-section of JET showing the plasma and main elements of the proposed pumped divertor.

APPENDIX 1.

THE JET TEAM

JET Joint Undertaking, Abingdon, Oxon, OX14 3EA, U.K.

J. M. Adams¹, F. Alladio⁴, H. Altmann, R. J. Anderson, G. Appuzzese, W. Bailey, B. Balet, D. V. Bartlett, L. R. Baylor²⁴, K. Behringer, A. C. Bell, P. Bertoldi, E. Bertolini, V. Bhatnagar, R. J. Bickerton, A. Boileau³, T. Bonicelli, S. J. Booth, G. Bosia, M. Botman, D. Boyd³¹, H. Brelen, H. Brinkschulte, M. Brusati, T. Budd, M. Bures, T. Businaro⁴, H. Buttgerit, D. Cacaut, C. Caldwell-Nichols, D. J. Campbell, P. Card, J. Carwardine, G. Celentano, P. Chabert²⁷, C. D. Challis, A. Cheetham, J. Christiansen, C. Christodouloupoulos, P. Chuilon, R. Claesen, S. Clement³⁰, J. P. Coad, P. Colestock⁶, S. Conroy¹³, M. Cooke, S. Cooper, J. G. Cordey, W. Core, S. Corti, A. E. Costley, G. Cottrell, M. Cox⁷, P. Cripwell¹³, F. Crisanti⁴, D. Cross, H. de Blank¹⁶, J. de Haas¹⁶, L. de Kock, E. Deksnis, G. B. Denne, G. Deschamps, G. Devillars, K. J. Dietz, J. Dobbing, S. E. Dorling, P. G. Doyle, D. F. Düchs, H. Duquenoy, A. Edwards, J. Ehrenberg¹⁴, T. Elevant¹², W. Engelhardt, S. K. Erents⁷, L. G. Eriksson⁵, M. Evrard², H. Falter, D. Flory, M. Forrest⁷, C. Froger, K. Fullard, M. Gadeberg¹¹, A. Galetsas, R. Galvao⁸, A. Gibson, R. D. Gill, A. Gondhalekar, C. Gordon, G. Gorini, C. Gormezano, N. A. Gottardi, C. Gowers, B. J. Green, F. S. Grigh, M. Gryzinski²⁶, R. Haange, G. Hammett⁶, W. Han⁹, C. J. Hancock, P. J. Harbour, N. C. Hawkes⁷, P. Haynes⁷, T. Hellsten, J. L. Hemmerich, R. Hemsworth, R. F. Herzog, K. Hirsch¹⁴, J. Hoekzema, W. A. Houlberg²⁴, J. How, M. Huart, A. Hubbard, T. P. Hughes³², M. Hugon, M. Huguet, J. Jacquinet, O. N. Jarvis, T. C. Jernigan²⁴, E. Joffrin, E. M. Jones, L. P. D. F. Jones, T. T. C. Jones, J. Källne, A. Kaye, B. E. Keen, M. Keilhacker, G. J. Kelly, A. Khare¹⁵, S. Knowlton, A. Konstantellos, M. Kovanen²¹, P. Kupschus, P. Lallia, J. R. Last, L. Lauro-Taroni, M. Laux³³, K. Lawson⁷, E. Lazzaro, M. Lennholm, X. Litaudon, P. Lomas, M. Lorentz-Gottardi², C. Lowry, G. Magyar, D. Maisonnier, M. Malacarne, V. Marchese, P. Massmann, L. McCarthy²⁸, G. McCracken⁷, P. Mendonca, P. Meriguet, P. Micozzi⁴, S. F. Mills, P. Millward, S. L. Milora²⁴, A. Moissonnier, P. L. Mondino, D. Moreau¹⁷, P. Morgan, H. Morsi¹⁴, G. Murphy, M. F. Nave, M. Newman, L. Nickesson, P. Nielsen, P. Noll, W. Obert, D. O'Brien, J. O'Rourke, M. G. Pacco-Düchs, M. Pain, S. Papastergiou, D. Pasini²⁰, M. Paume²⁷, N. Peacock⁷, D. Pearson¹³, F. Pegoraro, M. Pick, S. Pitcher⁷, J. Plancoulaine, J-P. Poffé, F. Porcelli, R. Prentice, T. Raimondi, J. Ramette¹⁷, J. M. Rax²⁷, C. Raymond, P-H. Rebut, J. Removille, F. Rimini, D. Robinson⁷, A. Rolfe, R. T. Ross, L. Rossi, G. Rupprecht¹⁴, R. Rushton, P. Rutter, H. C. Sack, G. Sadler, N. Salmon¹³, H. Salzmann¹⁴, A. Santagiustina, D. Schissel²⁵, P. H. Schild, M. Schmid, G. Schmidt⁶, R. L. Shaw, A. Sibley, R. Simonini, J. Sips¹⁶, P. Smeulders, J. Snipes, S. Sommers, L. Sonnerup, K. Sonnenberg, M. Stamp, P. Stangeby¹⁹, D. Start, C. A. Steed, D. Stork, P. E. Stott, T. E. Stringer, D. Stubberfield, T. Sugie¹⁸, D. Summers, H. Summers²⁰, J. Taboda-Duarte²², J. Tagle³⁰, H. Tamnen, A. Tanga, A. Taroni, C. Tebaldi²³, A. Tesini, P. R. Thomas, E. Thompson, K. Thomsen¹¹, P. Trevalion, M. Tschudin, B. Tubbing, K. Uchino²⁹, E. Usselmann, H. van der Beken, M. von Hellermann, T. Wade, C. Walker, B. A. Wallander, M. Walravens, K. Walter, D. Ward, M. L. Watkins, J. Wesson, D. H. Wheeler, J. Wilks, U. Willen¹², D. Wilson, T. Winkel, C. Woodward, M. Wykes, I. D. Young, L. Zannelli, M. Zarnstorff⁶, D. Zsche¹⁴, J. W. Zwart.

PERMANENT ADDRESS

1. UKAEA, Harwell, Oxon. UK.
2. EUR-EB Association, LPP-ERM/KMS, B-1040 Brussels, Belgium.
3. Institute National des Recherches Scientifique, Quebec, Canada.
4. ENEA-CENTRO Di Frascati, I-00044 Frascati, Roma, Italy.
5. Chalmers University of Technology, Göteborg, Sweden.
6. Princeton Plasma Physics Laboratory, New Jersey, USA.
7. UKAEA Culham Laboratory, Abingdon, Oxon. UK.
8. Plasma Physics Laboratory, Space Research Institute, Sao José dos Campos, Brazil.
9. Institute of Mathematics, University of Oxford, UK.
10. CRPP/EPFL, 21 Avenue des Bains, CH-1007 Lausanne, Switzerland.
11. Risø National Laboratory, DK-4000 Roskilde, Denmark.
12. Swedish Energy Research Commission, S-10072 Stockholm, Sweden.
13. Imperial College of Science and Technology, University of London, UK.
14. Max Planck Institut für Plasmaphysik, D-8046 Garching bei München, FRG.
15. Institute for Plasma Research, Gandhinagar Bhat Gujrat, India.
16. FOM Instituut voor Plasmafysica, 3430 Be Nieuwegein, The Netherlands.
17. Commissariat à l'Energie Atomique, F-92260 Fontenay-aux-Roses, France.
18. JAERI, Tokai Research Establishment, Tokai-Mura, Naka-Gun, Japan.
19. Institute for Aerospace Studies, University of Toronto, Downsview, Ontario, Canada.
20. University of Strathclyde, Glasgow, G4 ONG, U.K.
21. Nuclear Engineering Laboratory, Lapeenranta University, Finland.
22. JNICT, Lisboa, Portugal.
23. Department of Mathematics, Univeristy of Bologna, Italy.
24. Oak Ridge National Laboratory, Oak Ridge, Tenn., USA.
25. G.A. Technologies, San Diego, California, USA.
26. Institute for Nuclear Studies, Swierk, Poland.
27. Commissariat à l'Energie Atomique, Cadarache, France.
28. School of Physical Sciences, Flinders University of South Australia, South Australia 5042.
29. Kyushi University, Kasagu Fukuoka, Japan.
30. Centro de Investigaciones Energeticas Medioambientales y Techalógicas, Spain.
31. University of Maryland, College Park, Maryland, USA.
32. University of Essex, Colchester, UK.
33. Akademie de Wissenschaften, Berlin, DDR.